https://doi.org/10.5194/amt-2019-389
Preprint. Discussion started: 17 March 2020

Atmospheric Measurement Techniques Discussions

A mass spectrometric multiple soil-gas flux measurement system with portable high-resolution mass spectrometer MULTUM coupled to automatic chamber for continuous field observation

Noriko Nakayama[1], Yo Toma[2], Yusuke Iwai[3], Hiroshi Furutani[4], Toshinobu Hondo[5], Ryusuke Hatano[6], and Michisato Toyoda[1]

[1]Graduate School of Science, Osaka University, Toyonaka, Osaka 560-0043, Japan
[2]Faculty of Agriculture, Ehime University, Matsuyama, Ehime 790-8566, Japan
[3]Graduate School of Science, Osaka University, Toyonaka, Osaka 560-0043, Japan
[4]Center for Scientific Instrument Renovation and Manufacturing Support, Osaka University, Toyonaka, Osaka 560-0043, Japan
[5]Graduate School of Science, Osaka University, Toyonaka, Osaka 560-0043, Japan
[6]Research Faculty of Agriculture, Hokkaido University, Sapporo, Hokkaido 060-8589, Japan

Correspondence to: Noriko Nakayama (nnakayama@ess.sci.osaka-u.ac.jp)

Abstract. We developed a mass spectrometric soil-gas flux measurement system using a portable high-resolution multi-turn time-of-flight mass spectrometer, called MULTUM, combined with an automated soil-gas flux chamber for continuous field measurement of multiple gas concentrations. The developed system continuously measures concentrations of four different atmospheric gases (i.e., N_2O, CH_4, CO_2, and O_2), of which the concentrations range over six orders of magnitude at a time within a single gas sample. The measurements were performed every 2.5 min with analytical precisions (two standard deviations) of ±34 ppbv for N_2O, ±170 ppbv for CH_4, ±16 ppmv for CO_2, and ±0.60 vol% for O_2 at their atmospheric concentrations. The developed system was used for continuous field soil–atmosphere flux measurements of greenhouse gases (GHGs: N_2O, CH_4, and CO_2) and O_2 with 1 h resolution. The minimum quantitative fluxes (two standard deviations) were estimated through simulation as 70.2 μg N m^{-2} h^{-1} for N_2O, 139 μg C m^{-2} h^{-1} for CH_4, 11.7 mg C m^{-2} h^{-1} for CO_2, and 9.8 g O_2 m^{-2} h^{-1} (negative) for O_2, whereas the estimated minimum detectable fluxes (two standard deviations) were 17.2 μg N m^{-2} h^{-1} for N_2O, 35.4 μg C m^{-2} h^{-1} for CH_4, 2.6 mg C m^{-2} h^{-1} for CO_2, and 2.9 g O_2 m^{-2} h^{-1} for O_2. The developed system was deployed in the University Farm of the Ehime University (Matsuyama, Ehime, Japan) for a field observation over five days. Interestingly, an abrupt increase in N_2O flux from 70 to 682 μg N m^{-2} h^{-1} was observed a few hours after the first rainfall, whereas no obvious increase in the CO_2 flux was observed, although the temporal responses were different from those observed in a laboratory experiment. No abrupt N_2O flux change was observed in succeeding rainfalls. Continuous multiple-gas flux and concentration measurements can be a powerful tool for tracking and understanding of underlying biological and physicochemical processes in the soil through measuring more tracer gases, such as volatile organic carbon gases, reactive-nitrogen gases, and noble gases by taking advantage of the broad versatility of mass spectrometry in detecting broad range of gas species.

.

https://doi.org/10.5194/amt-2019-389
Preprint. Discussion started: 17 March 2020

Atmospheric Measurement Techniques Discussions

1 Introduction

Soil acts as either a source or sink of various atmospheric gases, including greenhouse gases (GHGs, *e.g.*, N_2O, CO_2, and CH_4) (*e,g.*, Oertel et al., 2016; Ito et al., 2018), oxygen (O_2) (Turcu et al., 2005, Huang et al., 2018), and biogenic volatile organic compounds (BVOCs) (Insam and Seewald, 2010; Peñuelas et al., 2014; Szog s et al., 2017, Mäki et al., 2019). The behaviors of either emitting or absorbing soil gases and their magnitudes are highly variable depending on the soil properties, such as soil biological and physicochemical characteristics in the soil, which are affected by environmental factors such as soil temperature, moisture, nutrients, pH level, rainfalls, etc. (Dick et al. 2001; Rowlings et al., 2012; Luo et al., 2013, Li et al., 2015, Arias-Navarro et al., 2017; Pärn et al., 2018). As soil conditions and environmental factors can vary within minutes to hours, the soil gases are also expected to vary in a similar time scale. Therefore, for accurate soil gas flux estimation, continuous measurement with high temporal resolution (*e.g.*, minutes) is essential to capture rapid variations and consider them to estimate average fluxes.

Although measurements of soil-atmosphere flux of GHGs have been extensively carried out due to their environmental impacts, other soil gas measurements have been less frequently conducted, in spite of these gases provide valuable biological and physicochemical insights in soil. For instance, measurement of O_2 concentration and flux are useful tracer to quantify the biological processes, since O_2 content in the soil is closely related to respiration of soil organisms and redox state in soil. It has been shown that the redox state in soil has a significant effect on biological GHGs generation processes, such as nitrification/denitrification (Hall et al., 2013, Heil et al., 2016). It has also been shown that soil microorganisms, soil fungi, and even plant roots produce BVOCs (e.g., Peñuelas et al., 2014). BVOCs seem to be not a simple intermediate/final products during metabolic cycles and microbial decomposition of organic matter, but play unique roles like signaling among microorganisms, fungi, and plant roots activities in soil (e.g., Peñuelas et al., 2014). The noble gases, being biologically and chemically inert, can be useful tracer if combined with biologically active soil gas since the noble gases can constrain physical processes, allowing the biological and physical components to be separated when considering the behavior of the biological active gas (Yang and Silver, 2012). The O_2/Ar has been used in an aquatic system to measure net O_2 productions (Kana et al., 1994; Nakayama et al., 2002). It is thus quite natural that simultaneous measurement of multiple soil gases with higher time resolution is quite advantageous for a better understanding of soil biological and physicochemical processes and gauging their environmental impacts. However, such simultaneous measurement of multiple soil gases is still challenging due to mostly lack of suitable measurement technology.

For the measurements of GHGs (CO_2, N_2O, CH_4, SF_6, and CO) and BVOCs in soil air, gas chromatography (GC) analysis has been extensively used, but with different measurement configurations and conditions suitable for each gas since these gases have different physicochemical properties and concentrations. GC coupled to electron capture detector (GC-ECD) has been used for N_2O and SF_6, while coupled to flame ion detector (GC-FID) has been used for carbon-containing gases, such as CH_4, CO_2, and CO including BVOCs. There are only few studies in which multiple gases in soil were analyzed by a single GC system, for instance, N_2O, CO_2, and CH_4 (Christiansen et al. 2015, Brannon et al., 2016), N_2O, CO_2, CH_4, and CO (van der

https://doi.org/10.5194/amt-2019-389
Preprint. Discussion started: 17 March 2020


Atmospheric Measurement Techniques Discussions

Laan et al., 2009), N_2O, CO_2, CH_4, CO, and SF_6 (Lopez et a., 2015). Although these studies claimed multiple soil gases measurement by a single GC system, in fact, several sub-GC systems optimized for different target gases (*e.g.*, GC-ECD, GC-FID with different columns and settings) were integrated into a single GC system. This complexity hinders the simultaneous measurement of multiple gases by the GC system at a time.

The recent advanced optical technique of cavity ring-down spectroscopy enables the simultaneous measurement of multiple GHGs (N_2O, CO_2, and CH_4) from soils, and it has been successfully applied for simultaneous gas flux measurements of multiple GHGs with temporal resolution of minutes to tens of minutes (Christiansen et al., 2015, Brannon et al., 2016; Lebegue, et al., 2016, Barba et al., 2019, Courtois et al., 2019). Despite the advantages of cavity ring-down spectroscopy, its application has been limited to GHGs since infrared absorption wavelengths of gases often overlap and undergo interference of other gases, and appropriate water vapor corrections are also required for accurate measurement. It is not yet applied for the measurement of trace gases (e.g., NO, SF_6), noble gases, and complex BVOCs in soil air.

Mass spectrometry (MS) provides high sensitivity and allows detecting a wide range of chemicals, being widely used for trace analysis of various compounds including multiple BVOCs measurement with proton-transfer reaction mass spectrometry (PTR-MS) (Veres et al., 2014, Mancuso et al., 2015, references in Penuelas et al., 2014). Still, the application of MS for simultaneous measurement of various GHGs has been limited due to the difficulty in mass resolution. In fact, CO_2 and N_2O, two important GHGs, have quite similar mass (43.989 and 44.001 u, respectively), and they are difficult to distinguish based on their ion peaks obtained from ordinary (e.g., quadruple) mass spectrometers. The independent detection of CO_2^+ and N_2O^+ by MS requires a mass resolving power above 10,000, corresponding to high-resolution spectrometry that is only achieved by mass spectrometers used in laboratory.

Only recently, simultaneous mass spectrometric field measurement of multiple GHGs has become feasible (Anan et al., 2014), after the introduction of a portable high-resolution multiturn time-of-flight mass spectrometer (MULTUM; Shimma et al., 2010), which has comparable dimensions to a desktop PC (215 × 545 × 610 mm, 45 kg) and high mass resolving power (30,000–50,000) for direct mass spectrometric separation of natural gas mixtures. Although MULTUM can resolve CO_2^+ and N_2O^+ ion peaks, it remains technically difficult to simultaneously measure the two GHGs and major gas components in the atmosphere (N_2 and O_2), whose concentrations in air substantially differ by more than six orders of magnitude (78.1%, 20.9%, 405 ppmv, and 330 ppbv for average atmospheric N_2, O_2, CO_2, and N_2O, respectively), due to the limited dynamic range of ion detection and signal acquisition. In addition, suppression in the electron ionization source causes major gases to restrict the ionization of other trace gases, undermining sensitivity to the latter. Even using MULTUM, these inherent restrictions in MS must be mitigated for simultaneous atmospheric gas measurement of N_2O, CH_4, CO_2, and O_2, of which the concentrations span over six orders of magnitude. Until now, the lack of field portable high-resolution MS and the technical difficulties of existing ion detectors and signal acquisition and processing have prevented the simultaneous field observation of even only multiple GHGs.

In this study, we combined the MULTUM field deployable multi-gas flux measurement system using a portable high-resolution mass spectrometer with a hybrid ion detection and signal processing technique to quantitatively and simultaneously

https://doi.org/10.5194/amt-2019-389
Preprint. Discussion started: 17 March 2020

Atmospheric Measurement Techniques Discussions

measure multiple gases with different concentrations over six orders of magnitude in a single measurement. We used the high-resolution MS system to measure the concentrations of N_2O, CH_4, CO_2, and O_2 every 2.5 min. The system was coupled with an automated open/closed chamber as the MULTUM–soil chamber system, to obtain hourly soil–atmosphere gas fluxes. In this paper, we detail the system and its characterization, including the simultaneous gas flux observations in both laboratory settings and an agricultural field.

2 Materials and methods

2.1 Simultaneous GHGs and O_2 measurement using MULTUM

Figure 1 illustrates the MULTUM–soil chamber system that comprises an automatic open/closed chamber, a sample/standard gas injection unit, and a mass spectrometer. The chamber was developed at Hokkaido University. The gas-tight lid of the custom chamber (0.25 × 0.37 m, inner diameter × height, 0.02 m^3 internal volume) is opened or closed by a DC motor attached to the chamber. The lid aperture timing is controlled using an FPGA platform (DE0-Nano-SoC Development Kit, Terasic, Hsinchu, Taiwan) with a Linux shell script through the "curl" command on a workstation. The system clocks of both the embedded Linux software and workstation are synchronized using the IEEE 1588-2008 protocol, obtaining a sub-microsecond time difference.

Soil gas in the chamber headspace continuously circulates through stainless-steel tubing (1/8 inch × 10 m, outer diameter × length) between the chamber and sample injection unit by an air pump (CM-15-12, Enomoto Micro Pump, Tokyo, Japan). The circulating soil gas continuously passes through a 100 µL sample loop (SL100CM, Valco Instruments, Houston, TX, USA) fitted to a port in a six-port auto valve (V_1) (SAV-VA-11-65, FLOM, Tokyo, Japan). When the headspace gas is analyzed with MULTUM (infiTOF-UHV, MSI Tokyo, Tokyo, Japan), the valve rotates and soil gas sample is injected into a porous layer open tubular capillary column with monolithic carbon layer (15 m × 0.320 mm, length × inner diameter, 3.0 µM; GS-CarbonPLOT, Agilent Technologies, Santa Clara, CA, USA) with carrier He gas stream (2.5 mL/min) for rough gas separation before feeding into MULTUM. Another six-port auto valve (V_2) (SAV-VA-11-65, FLOM, Tokyo, Japan) switches soil-gas sampling and standard gas injection for calibration. Sample gas injection occurs every 2.5 min, and both the sample and standard gas injections are controlled by the FPGA.

Although MULTUM has sufficient mass resolving power for complete separation of CO_2^+ and N_2O^+ ion peaks, we include the column to provide slight time lags between N_2/O_2, CO_2, and N_2O prior injection to the system to improve quantification. In fact, omitting the separation in time domain (20–60 s) causes several intrinsic MS problems. For instance, ionization of atmospheric trace gases with atmospheric major gases (e.g., N_2, O_2) restrict ionization of coexisting trace gases in the ion source, considerably increasing the detection limit of trace gases. In addition, the dynamic ranges of the ion detector and signal acquisition are limited, being about two to three orders of magnitude in total, thus impeding the simultaneous and accurate measurement of N_2O and CO_2 within a single gas sample, of which the concentrations differ by more than three orders of

https://doi.org/10.5194/amt-2019-389
Preprint. Discussion started: 17 March 2020


Atmospheric Measurement Techniques Discussions

magnitude. Therefore, we adopt a hybrid ion detection and signal processing technique that selects either waveform averaging or ion counting to detect ions with intensities differing by six orders of magnitude (Kawai et al., 2018).

In the conventional waveform averaging mode, much less abundant ions (e.g., N_2O^+) are difficult to be recognized as an ion peak because such low abundant ions are easily overwhelmed by background noise. In contrast, ion counting allows to detect scarce ions (Hoffmann and Stoobant, 2007) by regarding ion peaks above pre-defined threshold intensity (-10 mV in this study) as a single ion. However, counting loss occurs for abundant ions when two or more ions arrive at the detector within the minimum time resolution of the ion signal detection system. The present hybrid ion detection and signal processing scheme realizes the two detection modes by a single ion detector and recording system by selecting either waveform averaging or ion counting depending on the type of gas (at different periods from sample injection into the column) by changing the ion detector gain and real-time signal processing protocol (Hondo et al., 2017). Hence, the column is required to create small temporal separations for the detection of different target ions and select the appropriate measurement mode. For detection of CO_2^+, the ion detector voltage is set to 2400 V, and conventional waveform recording and averaging are conducted for the time-of-flight ion signal, whereas the voltage is set to 2650 V for the detection of O^+, CH_4^+, and N_2O^+, and real-time software thresholding (i.e., ion counting) is conducted for the acquired signal (Fig. 2). The optimized high-voltage settings of MULTUM for this study are listed in Table 1.

The gases injected into MULTUM are ionized by electron ionization at an electron acceleration voltage of 30 V, and the produced ions are mass-analyzed at a repetition rate of 1 kHz with 30 laps of circular ion flight, yielding a mass resolution of approximately 10,000. After the 30 laps, each ion is detected by an electron multiplier (ETP secondary electron multiplier 14882, ETP Ion Detect, Sydney, Australia). The ion signal from the ion detector is then amplified through a high-speed preamplifier (ORTEC 9301, Advanced Measurement Technology, Oak Ridge, TN, USA) and recorded and processed in real time with a high-speed 1 GS/s digitizer (U5303a, Keysight Technologies, Santa Rosa, CA, USA). Mass spectra are then transferred to a host PC (dual Intel 8-core/16-thread Xeon processor PC with Linux Debian 9.9 operating system). The data acquisition system is controlled by the QtPlatz open-source-software (https://github.com/qtplatz) with its plugin developed for the infiTOF system (Hondo et al., 2017, Jensen et al., 2017).

We calibrate the system with six different concentrations including blank gas (ultrapure N_2), which are prepared from mixed standard gases (mixture of N_2O, CH_4, and CO_2) and O_2 standard gas by diluting with ultrapure N_2 (>99.9995%, Takachiho Chemical Industrial). We use two certified standard gases (standard #1: N_2O, 279 ppbv; CH_4, 1.47 ppmv; CO_2, 421 ppmv in N_2; standard #2: N_2O, 1752 ppbv; CH_4, 2.97 ppmv; CO_2, 1705 ppmv in N_2; Sumitomo Seika Chemicals, Osaka, Japan) and O_2 standard gas (20.9% in N_2 balance gas; Takachiho Chemical Industrial, Tokyo, Japan). The gas mixing rates are adjusted using mass flow controllers (Model 8500 series, KOFLOC, Kojima Instruments, Kyoto, Japan). The mass flow controllers are calibrated using a soap film flowmeter (HORIBA STEC, Kyoto, Japan).

We continuously measured the standard gases using the developed MULTUM–soil chamber system and estimated the detection limits for N_2O, CO_2, CH_4, and O_2 based on the IUPAC criteria (Long and Winefordner, 1983) as follows:

https://doi.org/10.5194/amt-2019-389
Preprint. Discussion started: 17 March 2020

Atmospheric Measurement Techniques Discussions

$$LOD = k \cdot RSD/m, \quad (1)$$

where k is a constant that determines the confidence level (we set k = 3 for a confidence level above 99%), RSD is the standard deviation of the ion count or peak area of the target gas when measuring ultrapure N_2, and m is the slope of linear regression obtained from the measurement of the six above mentioned gas concentrations prepared from the standard gases and ultrapure N_2 based on 10 replicate measurements of each gas. The analytical precisions (one standard deviation, 1σ) of ±17 ppbv for N_2O, ±84 ppbv for CH_4, ±8.1 ppmv for CO_2, and ±0.30 vol% for O_2 were obtained at their atmospheric concentrations.

2.2 Flux measurement using MULTUM–soil chamber system

The fluxes of target soil gases are determined from the variation in the target gas concentration while the chamber is closed. During each flux measurement, 9 consecutive measurements over 20 min are carried out. A complete flux measurement is performed once per hour. In 0–20 min of flux measurement, the chamber is closed, whereas during the other 40 min, it remains open, and the standard #2 and atmospheric air measurements are conducted to monitor the MULTUM stability (Fig. 3). The standard gas measurement is repeated 5 times while atmospheric air measurement is repeated 10 times during the chamber open.

The fluxes of each of the four types of soil gases are calculated as (Minamikawa et al., 2015)

$$Flux = \frac{\Delta C}{\Delta t} \cdot \frac{V}{A} \cdot \rho \cdot \frac{273}{273+T} \cdot \alpha, \quad (2)$$

where $\Delta C/\Delta t$ is the concentration variation of the target gas during the flux measurement period, V is the chamber volume (in cubic meters, m^3), A is the chamber area (footprint in square meters, m^2), ρ is the gas density, T is mean air temperature inside the chamber (in degrees Celsius, °C), and α is a conversion factor to transform N_2O into N, and CH_4, CO_2 into C. We determine $\Delta C/\Delta t$ by applying linear regression to the data obtained from the 9 consecutive concentration measurements with the chamber closed.

Besides the flux measurement, we measure soil temperatures and moisture with a portable digital thermometer (EM50 Data Logger, METER Group, Pullman, WA, USA). We also monitor the air temperature inside the chamber and ambient temperature using a temperature data logger (Thermo Recorder TR-52i, T&D Corporation, Nagano, Japan).

The minimum detectable flux (MDF) of each soil gases can be estimated based on the derivations by Courtois et al. (2019) originally developed by Christiansen et al. (2015) and Nickerson (2016) as follows:

$$MDF_i = \left(\frac{1}{t_c} \cdot \frac{A_{a,i}}{\sqrt{n}}\right)\left(\frac{V \cdot P}{S \cdot R \cdot T}\right), \quad (3)$$

where $A_{a,i}$ is the analytical accuracy of MULTUM for gas i, t_c is the closure time of the soil flux chamber per flux measurement (20 min), n is the number of gas concentration measurements to calculate the gas flux (i.e., nine measurements), V is the volume of the flux chamber (0.018 m^3), P is the atmospheric pressure in kPa, S is the inner surface area of the flux chamber (0.049 m^2), R is the ideal gas constant (8.314 m^3 Pa K^{-1} mol^{-1}), and T is the ambient temperature surrounding the chamber in

https://doi.org/10.5194/amt-2019-389
Preprint. Discussion started: 17 March 2020


Atmospheric Measurement Techniques Discussions

K. We define the analytical accuracy ($A_{a,i}$) as the analytical precision (measurement uncertainty) of MULTUM for gas *i* and use the two standard deviations (2σ) obtained from 994 measurements of the gas in air.

2.3 Laboratory tests

We conducted laboratory flux measurement tests of N_2O, CH_4, CO_2, and O_2 with a soil sample collected at the University Farm of the Ehime University. The flux measurement cycle was the same as that used for field observation shown in Fig. 3 (chamber closed for 20 min, flux measurement with 9 concentration measurements every 2.5 min, and chamber open for the remaining 40 min). During the open chamber period, the standard gas and atmospheric air measurements were conducted for system calibration and verification. The soil was spared in a 60 L plastic container, and the automated flux chamber was placed on the soil. A urea solution ($CO(NH_2)_2$) was added to the soil (4 g of urea to 1 kg of soil) to promote N_2O generation. Then, the soil was air dried for a few days prior to flux measurement. After 22 h from the start of the laboratory flux measurement, a sufficient amount of water (3L) was sprayed to the soil for generating soil gases, and the flux measurement proceeded for 46 h.

2.4 Field observations

We deployed the developed MULTUM–soil chamber system in the University Farm of the Ehime University (Matsuyama-shi, Ehime, Japan) for a field observation over five days, September 3–8, 2018. The University Farm has been used for various agricultural production and soil studies (Toma, et al., 2019, Asagi and Ueno, 2009).

The automated flux chamber was placed on a ridge in the upland field, as shown in the left panel of Fig. 4. The field test was conducted during the fallow period (i.e., bare field condition). The soil pH, electric conductivity, and texture were 5.3, 34.0 µS cm^{-1}, and sandy loam (sand, 75.6%; silt, 10.6%; clay, 13.8%), respectively. On September 2, ammonium sulfate (150 kg N ha^{-1}) and dried cattle feces (10 Mg ha^{-1} of fresh weight) were applied and incorporated into the soil surface (0–15 cm depth). After plowing, the soil bulk density and porosity were 1.02 g cm^{-3} and 62.9%, respectively. Immediately after incorporation, the automated soil chamber was installed. The total carbon (C) and nitrogen (N) contents of the dried cattle feces were 36.1 and 2.08%, respectively. The other components of the MULTUM–soil chamber system (i.e., MULTUM platform, control, and data acquisition system) were installed at a nearby goat hut with room temperature of 27 ± 2 °C. Two 5 m long stainless-steel tubes (1/8 inch outer diameter) were used to connect the chamber and the six-port auto valve in the gas injection unit to circulate headspace gas within the chamber.

3 Results and discussion

3.1 Laboratory characterization of MULTUM–soil chamber system performance

We characterized the performance of the developed MULTUM–soil chamber system in the laboratory by introducing standard gases through the gas injection unit at six different concentrations, as described in section 2.3, following the procedure for the field observations. As shown in Fig. 5, MULTUM linearly responds to the gas concentrations during measurement, obtaining

https://doi.org/10.5194/amt-2019-389
Preprint. Discussion started: 17 March 2020

Atmospheric Measurement Techniques Discussions

coefficients of determination (R^2) of all the linear regression results above 0.996. The blank concentrations checked by introducing the ultrapure N_2 were very small compared to the atmospheric concentrations of target gases. The calculated detection limits were 12 ppbv for N_2O, 50 ppbv for CH_4, 13 ppmv for CO_2, and 0.68 vol% for O_2 based on the equation (2).

To verify the stability of the developed MULTUM–soil chamber system, we conducted a continuous measurement of atmospheric N_2O, CH_4, CO_2, and O_2 in the laboratory with the flux chamber open (Fig. 6). The set of N_2O, CH_4, CO_2, and O_2 measurements was repeated every 2.5 min over 42 h. In the laboratory, the room temperature remained stable (23 ± 1 °C) and the relative humidity was around 15% at the beginning of the measurement and increased to 30–33% after midnight of January 31, 2019. The atmospheric pressure during the laboratory measurement period ranged from 1005 to 1014 hPa. The variations of atmospheric N_2O, CH_4, CO_2, and O_2 measurements are shown as histograms in Fig. 7. As the distributions agree with Gaussian distributions plotted as dashed lines in Fig. 7, we calculated the standard deviations (2σ) of each gas from the measurements to obtain analytical accuracy $A_{a,i}$. The $A_{a,i}$ obtained from the atmospheric air measurements were ±34 ppbv for N_2O, ±170 ppbv for CH_4, ±16 ppmv for CO_2, and ±0.60 vol% for O_2. These variations may be subject to natural variabilities of atmospheric concentrations, however, we consider that they are instrumental variation since their frequency distributions nicely agreed with Gaussian distributions (Fig. 7) and the analytical precisions obtained from the measurements of standard#1 and O_2 standard in the laboratory (±17 ppbv for N_2O, ±84 ppbv for CH_4, ±8.1 ppmv for CO_2, and ±0.30 vol% for O_2, 1σ) almost corresponded to those obtained from the atmospheric air.

3.2 Laboratory flux measurement test

The temporal variation of measured gas concentrations with the chamber closed is shown in Fig. 8. Only data acquired with the chamber closed (flux measurement periods) is depicted for simplification, although the system stability verification and calibration were conducted with the chamber open. At 22 h, water (approximately 3 L) was sprayed on the soil surface as environmental perturbation resembling rainfall to reactivate the dormant soil biological processes. Immediately after water addition, the emission of N_2O and CO_2 began to change in different ways. Specifically, the CO_2 emission rapidly increased and reached its maximum 2 h after water addition and remained relatively high, whereas N_2O emission gradually increased until 20 h after water addition at a seemingly constant rate.

Such increases in soil CO_2 flux by rainfall or rewetting soil have been reported (Lee et al., 2002; Smith and Owens, 2010; Gelfand et al., 2015; Kostyanovsky et al., 2019), and enhanced microbial activity and population, boosted availability in carbon and nutrients by rewetting, or their assemblages are considered as possible causes (Fierer and Schimel, 2003; Iovieno and Bååth, 2008; Blazewicz et al., 2014). Similar N_2O flux increase upon rewetting soil have been reported (e.g., Nobre et al., 2001; Dobbie and Smith, 2003; Smith and Owens, 2010; Gelfand et al., 2015; Schwenke and Haigh, 2016; Leitner et al., 2017; Barba et al., 2019; Kostyanovsky et al., 2019), although very few research reported the simultaneous response of N_2O and CO_2 fluxes upon artificial watering (Smith and Owens, 2010; Gelfand et al., 2015; Kostyanovsky et al., 2019). Only Kostyanovsky et al. (2019) reported short-term flux changes of both CO_2 and N_2O upon simulated rainfall with a time resolution of 2 h. They showed that the simulated rainfall immediately triggered increases in both CO_2 and N_2O fluxes, but the increase in CO_2 flux

https://doi.org/10.5194/amt-2019-389
Preprint. Discussion started: 17 March 2020


Atmospheric Measurement Techniques Discussions

continued till about 3 h after the simulated rainfall, while that in N_2O flux continued till about 5 h after the simulated rainfall. In the present laboratory test, CO_2 and N_2O fluxes showed different temporal behaviors from those observed by Kostyanovsky et al. (2019), although observed N_2O flux change was similar to that observed by Leitner et al. (2017). We currently speculate that the slow increase in N_2O flux may reflect a slow building-up of nitrification and denitrification microorganisms after watering, although further studies, which apprehend both biological and physicochemical aspects of the soil gas formations, are necessary for better understanding.

3.3 Minimum detectable and minimum quantitative fluxes of GHGs and O_2

In Fig. 7, frequencies of atmospheric concentrations of N_2O, CH_4, CO_2, O_2 observed with the MULTUM–soil chamber system during the laboratory stability check (Fig. 6) are compiled as histograms. Their frequency distributions nicely agree with Gaussian distributions (plotted as dashed lines in Fig. 7), and thus their standard deviations are regarded as analytical accuracy ($A_{a,i}$) of the MULTUM–soil chamber system for each gas as described in section 3.1. We estimated the minimum detectable fluxes (MDFs) based on equation (3) using the $A_{a,i}$ for each gas, obtaining 17.2 μg N m^{-2} h^{-1}, 35.4 μg C m^{-2} h^{-1}, 2.6 mg C m^{-2} h^{-1}, and 2.9 g O_2 m^{-2} h^{-1} for N_2O, CH_4, CO_2, and O_2, respectively.

Although the MDF represents the minimum detectable flux, it is not a practical measure for reliable quantification of flux. Thereby, we evaluated minimum quantitative flux (MQF) for each gas as quantitatively reliable. Since flux is the rate of increase or decrease of gas concentration of interest in the closed chamber, we determine the flux by applying linear regression to every set of 9 consecutive gas concentration measurements with the closed chamber over 20 min. The accuracy of MQF depends on the variation of the slope of the regression line. As there is no formula for error/accuracy estimate in such slope determination, we conducted a simulation study to characterize the MQF considering the measurement error.

We first defined a true flux value of the gas for model simulation assuming that the flux remained constant during the chamber closed period. Based on the defined true flux value and chamber dimension, "true" gas concentrations to be measured in the chamber over time during the chamber closed were calculated. To simulate realistic observation, random measurement error based on the standard deviation derived from the atmospheric gas measurements (see section 3.1) was intentionally added to the predefined "true" gas concentrations during the chamber closed. The simulated 9 consecutive observation data was then used for flux determination with the linear regression analysis, whose results were further characterized for the MQF estimation. For each defined flux value, 10,000 sets of flux measurements were simulated, and the 10,000 corresponding slopes were obtained, and standard deviations of the slopes were characterized. The simulation was conducted on a scientific graphical data processing software (Igor Pro, WaveMetrics, Lake Oswego, OR, USA) and the random measurement error was generated with a built-in Gaussian distribution noise generator.

Figures 9(a) to (d) show the relationship between true flux and calculated fluxes from a simulation. The error bars in the figures represent error ranges of fluxes (2σ) determined from the simulation. The average fluxes determined by the simulation were almost equal to their corresponding true fluxes, and the errors were relatively constant. Here, we defined the MQF as the flux when the true flux is equal to the error (2σ) of the corresponding simulated flux. We obtained MQFs of 70.2 μg N m^{-2} h^{-1}

https://doi.org/10.5194/amt-2019-389
Preprint. Discussion started: 17 March 2020


Atmospheric Measurement Techniques Discussions

for N_2O, 139 μg C m^{-2} h^{-1} for CH_4, 11.7 mg C m^{-2} h^{-1} for CO_2, and 9.8 g O_2 m^{-2} h^{-1} (negative flux) for O_2. We regarded observed fluxes below the MQFs as qualitatively uncertain and did not use them in subsequent data analyses for this study.

We also conducted data quality checks for the filed observation flux data using coefficients of determination (R^2) in the linear regression analysis for 9 consecutive concentration measurements during the chamber closed. Fig. 10 shows the relationships between observed fluxes and the corresponding R^2 in the N_2O and CO_2 flux derivation during field flux observation at the Ehime University. The R^2 was approximately 0.4 at its MQF (70.2 μg N m^{-2} h^{-1}) in the N_2O flux observation. The data with R_2 = 0.4 on its linear regression analysis is generally regarded that the data has a statistically significant correlation, supporting that the MQF is a reasonable metric for reliable quantification. In the field N_2O flux measurement, R^2 increased with the observed flux increased, indicating that improvement of quality in N_2O measurement (i.e., detection limit and sensitivity) is desirable for more accurate determination, in particular, under low N_2O flux condition. All CO_2 flux measurements showed $R^2 > 0.9$, indicating that the present system is accurate enough for the CO_2 flux determination. The observed fluxes of CH_4 and O_2 during the field study were usually below their MQFs and not discussed in this study. Notable CH_4 flux well above the MQF was observed in the same field but during springtime, and may be discussed in a separate paper.

3.4 Field observation

We conducted the field flux observation at the University Farm of the Ehime University over five days in September 2018. We only report the N_2O and CO_2 flux results because we observed fluxes below the MQFs for CH_4 and O_2 in this field observation, as mentioned above. The N_2O fluxes remained mostly below 300 μg N m^{-2} h^{-1} and were generally dependent on soil moisture, which substantially affects the production, consumption, and atmospheric exchange of GHGs (Davidson and Swank, 1986, Dobbie and Smith, 2003, Liebig et al. 2005, Ellert and Janzen 2008, Sainju et al. 2012). An interesting event was observed in the N_2O flux on September 4. The N_2O flux abruptly increased from 70 to 682 μg N m^{-2} h^{-1} within a few hours after the rainfall, while a sudden drop in CO_2 flux was observed. These observed responses exhibit sharp contrast with our laboratory flux measurement test, in which CO_2 flux showed a rapid increase while N_2O flux showed a slow sustained increase upon water spraying (Fig. 8). Various studies have reported increased N_2O flux after rainfall (Nobre et al., 2001; Dobbie and Smith, 2003; Smith and Owens, 2010; Gelfand et al., 2015; Schwenke and Haigh, 2016; Leitner et al., 2017; Barba et al., 2019; Kostyanovsky et al., 2019) and similar increased CO_2 flux after rainfall has been reported (Lee et al., 2002; Smith and Owens, 2010; Gelfand et al., 2015; Kostyanovsky et al., 2019). However, no short-term responses of CO_2 and N_2O fluxes, similar to our observation upon rainfall, were reported. The other two heavier rainfalls also occurred on September 5 and 7; however, the N_2O flux shows no obvious increase like that after the first rainfall. The different responses in N_2O flux may reflect the complexity in microbial and nutrient dynamics initiated in the soil upon rainfall (e.g., Gordon et al., 2008; Blazewicz et al., 2014), although further detailed studies, which apprehend both biological and physicochemical aspects of the soil gas formations, are necessary to describe the causes of the response. The CO_2 flux, in contrast, remained constant except during rainfall periods, in which an abrupt decrease and quick recovery within several hours of the flux occurred. Possible

https://doi.org/10.5194/amt-2019-389
Preprint. Discussion started: 17 March 2020


Atmospheric Measurement Techniques Discussions

explanations may be a suppression of CO_2 permeation within the soil column by a capping effect of wet soil and different vertical distributions within the soil column, although these explanations are feasible but require further investigation.

3.5 Future perspectives

The present results clearly show the advantage of continuous (hourly) multiple-soil gas flux measurements to capture sporadic events and contrasting temporal behaviors and responses from different GHGs. Tracking unique and contrasting behaviors and responses against environmental perturbations should aid further understanding of underlying biological and physicochemical processes in soil. The advantage can be further enhanced by expanding the range of gas measurements beyond GHGs as tracers. MS can analyze any ionizable compounds, such as BVOCs and inorganic gases, noble gases, hydrogen, NO, H_2S, N_2, O_2, which is quite useful for a comprehensive understanding of biological, chemical, and physical processes occurring in soil and environment. Further improvement in detection limit and analytical precision are desired for the further gas measurement beyond current GHGs measurement and more accurate observation. We consider that the improvement in the detection limit by one order of magnitude can be relatively easy by retrofitting a larger vacuum pump to the MULTUM (from 50 l/sec to 250 l/sec) and using a flux chamber with lower height (from 0.37 m to 0.2 m). Also, applying waveform averaging mode for the measurement of more abundant O_2^+ instead of current ion counting mode for O^+ should improve the analytical precession of O_2 concentration measurement, and O_2 flux measurement will be feasible. Coupling of proton transfer reaction (PTR) ionization sources with the MULTUM also makes it easier to observe BVOCs concentrations and soil-atmosphere fluxes. We expect that with these further improvements, more accurate and more multiple gas flux measurements will provide deeper insights on the soil's biological and physicochemical processes and lead to their more comprehensive understandings.

4 Conclusion

We developed a field-deployable MS-based multi-gas flux measurement system utilizing a portable high-resolution mass spectrometer (MULTUM) combined with an automated soil-gas chamber. To overcome the inherent limitations in MS, atmospheric air samples were separated into each component over short periods with a short gas separation column, and a hybrid ion detection and signal processing technique was utilized to ensure a wide dynamic range for quantitative and simultaneous measurement of multiple gases, which concentrations differ by six orders of magnitude. We continuously observed atmospheric gases every 2.5 min and obtained analytical precisions (2σ) of ±34 ppbv for N_2O, ±170 ppbv for CH_4, ±16 ppmv for CO_2, and ±0.60 vol% for O_2. Soil–atmosphere gas fluxes were determined through sets of nine consecutive measurements with the chamber closed for 20 min. The estimated minimum quantitative fluxes (MQFs) for GHGs were 70.2 μg N m^{-2} h^{-1} for N_2O, 139 μg C m^{-2} h^{-1} for CH_4, 11.7 mg C m^{-2} h^{-1} for CO_2, and 9.8 g O_2 m^{-2} h^{-1} (negative) for O_2. We also conducted a continuous (hourly) field observation in an upland field over five days. During the field observation, N_2O and CO_2 fluxes exhibited different temporal changes. Specifically, a rapid and sustained increase in N_2O flux occurred after the first rainfall without notable variation in CO_2 flux, although a laboratory flux measurement test with an artificial field showed

https://doi.org/10.5194/amt-2019-389
Preprint. Discussion started: 17 March 2020


Atmospheric Measurement Techniques Discussions

a simultaneous increase in both CO_2 and N_2O but with different temporal responses. The observed unique temporal behaviors show the advantage of continuous and simultaneous multiple-gas flux measurement for the elucidating underlying soil biological and physicochemical processes. The privilege of a highly sensitive and wider range of detectable compounds of MS-based multiple gas measurement, including BVOCs, reactive-nitrogen gases, and noble gases, should provide deeper insights into soil microbiological ecosystems, physicochemical processes, and their responses to environmental perturbations.

Data Availability. Data are available upon request.

Author contributions. NN led this research project and conducted a major part of the study. YT coordinated the field campaign, assisted with the field flux measurement, and provided valuable feedback and advice for the field measurements. YI assisted in conducting a field test. TH constructed the hybrid ion detection and signal processing technique as well as the data analysis tools. HF developed a prototype of the multiple-gas measurement, MULTUM, system. RH and MT created the conceptual framework of this study. All authors discussed the results and contributed to the preparation of the final manuscript.

Competing interests. The authors declare that they have no conflict of interest.

Acknowledgments. We thank the supporting staff at the University Fam in Ehime University for their assistance during the field observation. We also thank Hisanori Matsuoka for his assistance in developing and optimizing the electrical systems, and Toshio Ichihara for the fabrication of the soil chamber. This work was supported by JSPS Challenging Research (Exploratory) under grant number 17K20044.

Review statement. This paper was edited by Christian Brümmer and reviewed by two anonymous referees.

References

Anan, T., Shimma, S., Toma, Y., Hashidoko, Y., Hatano, R., and Toyoda, M.: Real time monitoring of gases emitted from soils using a multi-turn time-of-flight mass spectrometer “MULTUM-S II”, Environ. Sci-Proc Imp., 16, 2752–2757, https://doi.org/10.1039/C4EM00339J, 2014.

https://doi.org/10.5194/amt-2019-389
Preprint. Discussion started: 17 March 2020


Atmospheric Measurement Techniques Discussions

Arias-Navarro, C., Díaz-Pinés, E., Klatt, S., Brandt, P., Rufino, M. C., Butterbach-Bahl, K., and Verchot, L. V.: Spatial variability of soil N_2O and CO_2 fluxes in different topographic positions in a tropical mountain forest in Kenya, J. Geophys. Res. Biogeosci., 122, 514–527, https://doi.org/10.1002/2016JG003667, 2017.

Asagi, N. and Ueno, H.: Nitrogen dynamics in paddy soil applied with various ^{15}N-labelled green manures, Plant Soil, 322, 251–262, https://doi.org/10.1007/s11104-009-9913-4, 2009.

Barba, J., Poyatos, R., and Vargas, R.: Automated measurements of greenhouse gases fluxes from tree stems and soils: magnitudes, patterns and drivers, Sci. Rep., 9, 1–13, https://doi.org/10.1038/s41598-019-39663-8, 2019.

Blazewicz, S. J., Schwartz, E. and Firestone, M. K.: Growth and death of bacteria and fungi underlie rainfall-induced carbon dioxide pulses from seasonally dried soil, Ecology, 95, 1162-1172, https://doi.org/10.1890/13-1031.1, 2014.

Brannon, E. Q., Moseman-Valtierra, S. M., Rella, C. W., Martin, R. M., Chen, X., and Tang, J.: Evaluation of laser-based spectrometers for greenhouse gas flux measurements in coastal marshes, Limnol. Oceanogr-Meth., 14, 466–476, https://doi.org/10.1002/lom3.10105, 2016.

Christiansen, J. R., Outhwaite, J., and Smukler, S. M.: Comparison of CO_2, CH_4 and N_2O soil-atmosphere exchange measured in static chambers with cavity ring-down spectroscopy and gas chromatography. Agric. For. Meteorol., 211–212, 48–57, https://doi.org/10.1016/j.agrformet.2015.06.004, 2015.

Courtois, E. A., Stahl, C., Burban, B., Van den Berge, J., Berveiller, D., Bréchet, L., Soong, J. L., Arriga, N., Peñuelas, J., and Janssens, I. A.: Automatic high-frequency measurements of full soil greenhouse gas fluxes in a tropical forest, Biogeosciences, 16, 785–796, https://doi.org/10.5194/bg-16-785-2019, 2019.

Davidson, E. A. and Swank, W. T.: Environmental parameters regulating gaseous nitrogen losses from two forested ecosystems via nitrification and denitrification, Appl. Environ. Microbiol., 52, 1287–1292, PMID: 16347234, PMCID: PMC239223, 1986.

Dick, L, Skiba, U. and Wilson, L.: The effect of rainfall on NO and N_2O emissions from Ugandan agroforest soils. Phyton-Annales Rei Botanicae, 41, 73–80, http://nora.nerc.ac.uk/id/eprint/1023, 2001.

Dobbie, K. E. and Smith, K. A.: Nitrous oxide emission factors for agricultural soils in Great Britain: the impact of soil water-filled pore space and other controlling variables, Glob. Change Biol., 9, 204-218, https://doi.org/10.1046/j.1365-2486.2003.00563.x, 2003.

Ellert, B. H. and Janzen, H. H.: Nitrous oxide, carbon dioxide and methane emissions from irrigated cropping systems as influenced by legumes, manure and fertilizer. Can. J. Soil Sci., 88, 207–217, https://doi.org/10.4141/CJSS06036, 2008.

Fierer, N. and Schimel, J. P.: A Proposed Mechanism for the Pulse in Carbon Dioxide Production Commonly Observed Following the Rapid Rewetting of a Dry Soil, Soil Sci. Soc. Am. J., 67, 798–805, https://doi.org/10.2136/sssaj2003.0798, 2013.

Gelfand, I., Cui, M., Tang, J. and Robertson, G.P.: Short-term drought response of N_2O and CO_2 emissions from mesic agricultural soils in the US Midwest, Agric. Ecosyst. Environ. 212, 127–133, https://doi.org/10.1016/j.agee.2015.07.005, 2015.

https://doi.org/10.5194/amt-2019-389
Preprint. Discussion started: 17 March 2020

Gordon, H., Haygarth, P. M., and Bardgett, R. D.: Drying and rewetting effects on soil microbial community composition and nutrient leaching, Soil Biol. Biochem., 40, 302–311, https://doi.org/10.1007/s00248-010-9723-5, 2008.

Hall, S. J., McDowell, W. H. and Silver, W. L.: When Wet Gets Wetter: Decoupling of Moisture, Redox Biogeochemistry, and Greenhouse Gas Fluxes in a Humid Tropical Forest Soil, Ecosystems, 16, 576–589, https://doi.org/10.1007/s10021-012-9631-2.

Heil, J., Vereecken, H. and Brüggemann, N.: A review of chemical reactions of nitrification intermediates and their role in nitrogen cycling and nitrogen trace gas formation in soil. Eur. J. Soil Sci., 67, 23–39, https://doi.org/10.1111/ejss.12306, 2016.

Hoffmann, E. and Stroobant, V.: Mass Spectrometry Principles and Applications, 3rd edition, Wiley, Chichester, England, 2007.

Hondo, T., Jensen, K. R., Aoki, J., and Toyoda, M.: A new approach for accurate mass assignment on a multi-turn time-of-flight mass spectrometer, Eur. J. Mass Spectrom., 23, 385–392, https://doi.org/10.1177/1469066717723755, 2017.

Huang, J., Huang, J., Liu, X., Li, C., Ding, L. and Yu, H.: The global oxygen budget and its future projection, Sci. Bull., 63, 1180–1186, https://doi.org/10.1016/j.scib.2018.07.023, 2018.

Insam, H., and Seewald, M. S.: Volatile organic compounds (VOCs) in soils, Biol. Fert. Soils, 46, 199–213, https://doi.org/10.1007/s00374-010-0442-3, 2010.

Iovieno, P. and Bååth, E.: Effect of drying and rewetting on bacterial growth rates in soil, FEMS microbiology ecology, 65, 400–7, https://doi.org/10.1111/j.1574-6941.2008.00524.x, 2008.

Ito, A., Nishina, K., Ishijima, K., Hashimoto, S., and Inatomi, M.: Emissions of nitrous oxide (N_2O) from soil surfaces and their historical changes in East Asia: a model-based assessment, Prog. Earth Planet. Sci., 5, 55, https://doi.org/10.1186/s40645-018-0215-4, 2018.

Jensen, K. R., Hondo, T., Sumino, H., and Toyoda, M.: Instrumentation and method development for on-site analysis of helium isotopes, Anal. Chem., 89, 7535–7540, https://doi.org/10.1021/acs.analchem.7b01299, 2017.

Kana, T., Darkangelo, C., Hunt, M., Oldham, J., Bennett, G. and Cornwell, J.: Membrane inlet mass spectrometer for rapid high-precision determination of N_2, O_2, and Ar in environmental water samples, Anal. Chem., 66, 4166–4170, https://doi.org/10.1021/ac00095a009, 1994.

Kawai, Y., Hondo, T., Jensen, K. R., Toyoda, M., and Terada, K: Improved quantitative dynamic range of time-of-flight mass spectrometry by simultaneously waveform-averaging and ion-counting data acquisition, J. Am. Soc. Mass Spectrom., 29, 1403–1407, https://doi.org/10.1007/s13361-018-1967-1, 2018.

Kostyanovsky, K. I., Huggins, D. R., Stockle, C. O., Morrow, J. G. and Madsen, I. J.: Emissions of N_2O and CO_2 Following Short-Term Water and N Fertilization Events in Wheat-Based Cropping Systems, Frontiers in Ecology and Evolution, 7, 63, https://doi.org/10.3389/fevo.2019.00063, 2019.

Laan, S. V. D, Neubert, R. E. M. and Meijer, H. A. J.: A single gas chromatograph for accurate atmospheric mixing ratio measurements of CO_2, CH_4, N_2O, SF_6 and CO, Atmos. Meas. Tech., 2, 549–559, https://doi.org/10.5194/amt-2-549-2009.

445 Lebegue, B., Schmidt, M., Ramonet, M., Wastine, B., Yver Kwok, C., Laurent, O., Belviso, S., Guemri, A., Philippon, C., Smith, J., and Conil, S.: Comparison of nitrous oxide (N_2O) analyzers for high-precision measurements of atmospheric mole fractions, Atmos. Meas. Tech., 9, 1221–1238, https://doi.org/10.5194/amt-9-1221-2016, 2016.

Lee, M., Nakane, K., Nakatsubo, T., Mo, W. and Koizumi, H.: Effects of rainfall events on soil CO_2 flux in a cool temperate deciduous broad-leaved forest. Ecological Research, 17, 401–409. https://doi.org/10.1046/j.1440-1703.2002.00498.x,
450 2002.

Leitner S., Minixhofer P., Inselsbacher E., Keiblinger K.M., Zimmermann M. and Zechmeister-Boltenstern S.: Short-term soil mineral and organic nitrogen fluxes during moderate and severe drying–rewetting events. Appl. Soil Ecol., 114, 28–33, https://doi.org/10.1016/j.apsoil.2017.02.014, 2017.

Li, X., Ishikura, K., Wang, C., Yeluripati, J., and Hatano, R.: Hierarchical Bayesian models for soil CO_2 flux using soil texture:
455 a case study in central Hokkaido, Japan, Soil Sci. Plant Nutr., 61, 116–132, https://doi.org/10.1080/00380768.2014.978728, 2015.

Liebig, M. A., Morgan, J. A., Reeder, J. D., Ellert, B. H., Gollany, H. T., and Schuman, G. E.: Greenhouse gas contributions and mitigation potential of agricultural practices in northwestern USA and western Canada, Soil Tillage Res., 83, 25–52, https://doi.org/10.1016/j.still.2005.02.008, 2005.

460 Long, G. L. and Winefordner, J. D.: Limit of detection. A closer look at the IUPAC definition. Anal. Chem. 55, 712A– 724A, https://doi.org/10.1021/ac00258a001, 1983.

Lopez, M., Schmidt, M., Ramonet, M., Bonne, J.-L., Colomb, A., Kazan, V., Laj, P. and Pichon, J.-M.: Three years of semicontinuous greenhouse gas measurements at the Puy de Dôme station (central France), Atmos. Meas. Tech. 8, 3941–3958, https://doi.org/10.5194/amt-8-3941-2015, 2015.

465 Luo, G. J., Kiese, R., Wolf, B., and Butterbach-Bahl, K.: Effects of soil temperature and moisture on methane uptake and nitrous oxide emissions across three different ecosystem types, Biogeoscien, ces, 10, 3205–3219, https://doi.org/10.5194/bg-10-3205-2013, 2013.

Mäki, M. J., Aalto, J., Hellén, H., Pihlatie, M., and Bäck, J.: Interannual and seasonal dynamics of volatile organic compound fluxes from the boreal forest floor, Front. Plant Sci., 10, 1–14, https://doi.org/10.3389/fpls.2019.00191, 2019.

470 Mancuso, S., Taiti, C., Bazihizina, N., Costa, C., Menesatti, P., Giagnoni, L., Arenella, M., Nannipieri, P. and Renella, G.: Soil volatile analysis by proton transfer reaction-time of flight mass spectrometry (PTR–TOF–MS), Appl. Soil Ecol., 86, 182–191, https://doi.org/10.1016/j.apsoil.2014.10.018, 2015.

Nakayama, N., Watanabe, S. and Tsunogai, S.: Nitrogen, oxygen and argon dissolved in the northern North Pacific in early summer, J. Oceanogr., 58, 775–785, https://doi.org/10.1023/A:1022810827059, 2002.

475 Nickerson, N.: Evaluating Gas Emission Measurements Using Minimum Detectable Flux (MDF), Eosense, Dartmouth, Canada, https://doi.org/10.13140/RG.2.1.4149.2089, 2016.

https://doi.org/10.5194/amt-2019-389
Preprint. Discussion started: 17 March 2020


Atmospheric Measurement Techniques Discussions

Nobre, A., Keller, M., Crill, P. and Harriss, R.: Short-term nitrous oxide profile dynamics and emissions response to water, nitrogen and carbon additions in two tropical soils, Biol. Fertil. Soils, 34, 363–373, https://doi.org/10.1007/s003740100396, 2001.

Minamikawa, K., Tokida, T., Sudo, S., Padre, A., and Yagi, K.: Guidelines for Measuring CH_4 and N_2O Emissions from Rice Paddies by a Manually Operated Closed Chamber Method, National Institute for Agro-Environmental Sciences, Tsukuba, Japan, 2015.

Oertel, C., Matschullat, J., Zurbaa, K., Zimmermann, F., and Erasmi, S.: Greenhouse gas emissions from soils—a review, Geochemistry, 76, 327–352, https://doi.org/10.1016/j.chemer.2016.04.002, 2016.

Pärn J., Verhoeven, J. T., Butterbach-Bahl, K., Dise, N. B., Ullah, S., Aasa, A., Egorov, S., Espenberg, M., Järveoja, J., Jauhiainen, J., Kasak, K., Klemedtsson, L., Kull, A., Laggoun-Défarge, F., Lapshina, E. D., Lohila, A., Lõhmus, K., Maddison, M., Mitsch, W. J., Müller, C., Niinemets, Ü., Osborne, B., Pae, T., Salm, J. O., Sgouridis, F., Sohar, K., Soosaar, K., Storey, K., Teemusk, A., Tenywa, M. M., Tournebize, J., Truu, J., Veber, G., Villa, J. A., Zaw, S. S., and Mander, Ü.: Nitrogen-rich organic soils under warm well-drained conditions are global nitrous oxide emission hotspots, Nat. Commun., 9, 1–8, https://doi.org/10.1038/s41467-018-03540-1, 2018.

Peñuelas, J., Asensio, D., Tholl, D., Wenke, K., Rosenkranz, M., Piechulla, B. and Schnitzler, J. P.: Biogenic volatile emissions from the soil. Plant, Cell Environ., 37, 1866–1891, https://doi.org/10.1111/pce.12340, 2014.

Rowlings, D. W., Grace, P. R., Kiese, R., and Weier, K. L.: Environmental factors controlling temporal and spatial variability in the soil-atmosphere exchange of CO_2, CH_4 and N_2O from t, Glob. Change Biol., 18, 726–738, https://doi.org/10.1111/j.1365-2486.2011.02563.x, 2012.

Sainju, U. M., Stevens, W. B., Caesar-TonThat, T., and Liebig, M. A.: Soil greenhouse gas emissions affected by irrigation, tillage, crop rotation, and nitrogen fertilization. J. Environ. Qual., 41, 1774–1786, https://doi.org/10.2134/jeq2012.0176, 2012.

Schwenke, G. D. and Haigh, B. M.: The interaction of seasonal rainfall and nitrogen fertiliser rate on soil N_2O emission, total N loss and crop yield of dryland sorghum and sunflower grown on sub-tropical Vertosols, Soil Research, 54, 604–618, https://doi.org/10.1071/SR15286, 2016.

Shimma, S., Nagao, H., Aoki, J., Takahashi, K., Miki S., and Toyoda, M.: Miniaturized high-resolution time-of-flight mass spectrometer MULTUM-S II with an infinite flight path, Anal. Chem., 82, 8456–8463, https://doi.org/10.1021/ac1010348, 2010.

Smith, D. R. and Owens, P. R.: Impact of time to first rainfall event on greenhouse gas emissions following manure applications. Commun. Soil Sci. Plant Anal., 41, 1604–1614, https://doi.org/10.1080/00103624.2010.485240, 2010.

Szogs, S., Arneth, A., Anthoni, P., Doelman, J. C., Humpenöder, F., Popp, A., Pugh, T. A., and Stehfest, E.: Impact of LULCC on the emission of BVOCs during the 21st century, Atmos. Environ., 165, 73–87, https://doi.org/10.1016/j.atmosenv.2017.06.025, 2017.

https://doi.org/10.5194/amt-2019-389
Preprint. Discussion started: 17 March 2020

Turcu, V. E., Jones, S. B. and Or, D.: Continuous Soil Carbon Dioxide and Oxygen Measurements and Estimation of Gradient-Based Gaseous Flux. Vadose Zone J., 4, 1161–1169, https://doi.org/10.2136/vzj2004.0164, 2005.

Toma, Y., Sari, N. N., Akamatsu, K., Oomori, S., Nagata, O., Nishimura, S., Purwanto, B. H., and Ueno, H.: Effects of green manure application and prolonging mid-season drainage on greenhouse gas emission from paddy fields in Ehime, Southwestern Japan. Agriculture, 9, 1–17, https://doi.org/10.3390/agriculture9020029, 2019.

Veres, P. R., Behrendt, T., Klapthor, A., Meixner, F. X. and Williams, J.: Volatile Organic Compound emissions from soil: using Proton-Transfer-Reaction Time-of-Flight Mass Spectrometry (PTR-TOF-MS) for the real time observation of microbial processes, Biogeosciences Discuss., 11, 12009–12038, https://doi.org/10.5194/bgd-11-12009-2014, 2014.

Yang, W. H. and Silver, W. L.: Application of the N_2/Ar Technique to Measuring Soil-Atmosphere N_2 Fluxes: Measuring Soil Surface N_2 Fluxes, Rapid Commun. Mass Spectrom., 26, 449–59, https://doi.org/10.1002/rcm.6124, 2012.

https://doi.org/10.5194/amt-2019-389
Preprint. Discussion started: 17 March 2020

Atmospheric Measurement Techniques Discussions

Table 1. Elapsed time since sample injection and corresponding adjustment of ion detector voltage in MULTUM to perform hybrid ion detection and signal processing (waveform averaging or ion counting) for specific target ions.

GC elapsed time [sec]	Detector voltage [V]	Target gas	*m/z*	Data acquisition method
0	1400	-	-	-
48	2650	O^+	15.994	ion-counting
		CH_4^+	16.031	
73	2400	CO_2^+	44.001	waveform averaging
96	2650	N_2O^+	43.989	ion-counting
125	1400	-	-	-

https://doi.org/10.5194/amt-2019-389
Preprint. Discussion started: 17 March 2020

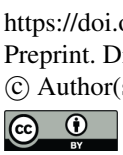

Atmospheric Measurement Techniques Discussions

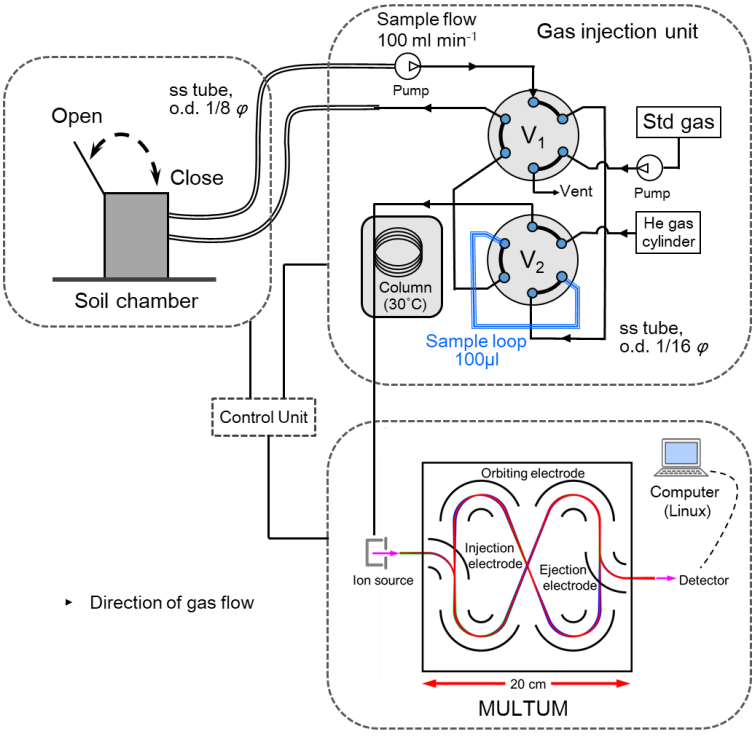

Figure 1. Schematic diagram of developed mass spectrometric multiple soil-gas flux measurement system with portable high-resolution multiturn time-of-fright mass spectrometer (MULTUM) coupled with automated soil-gas flux chamber. The headspace gas in the chamber continuously circulates through a gas injection unit with stainless-steel tubing. In gas analysis, sample air in the sample loop is injected into a capillary column for rough gas separation before analyzing the gases with MULTUM. (o.d., outer diameter; ss, stainless steel; Std, standard)

https://doi.org/10.5194/amt-2019-389
Preprint. Discussion started: 17 March 2020

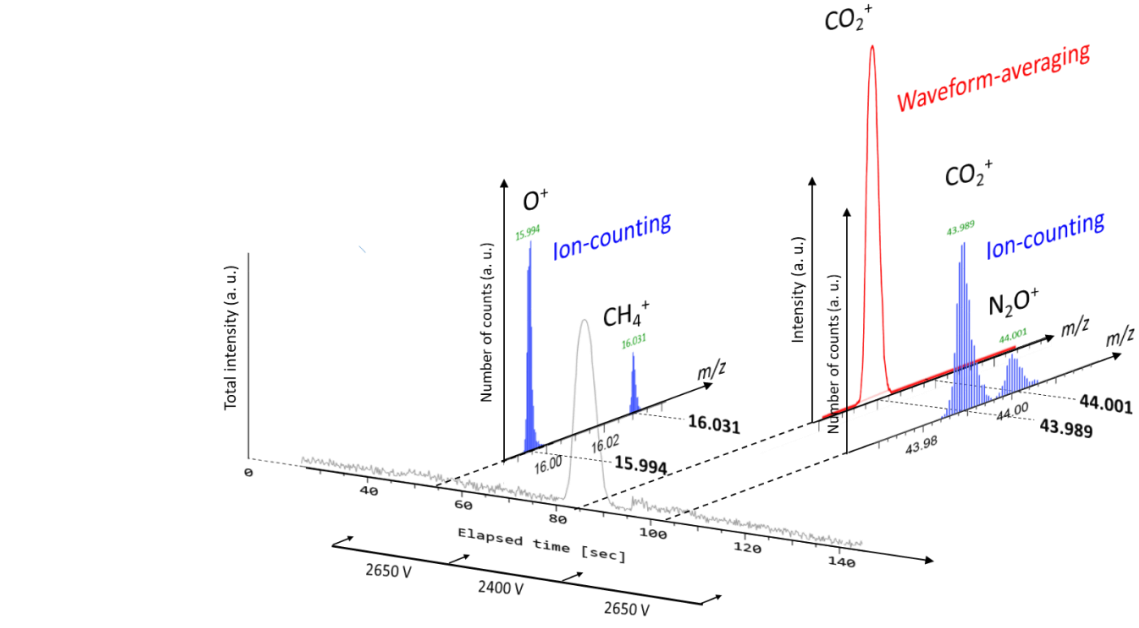

Figure 2. Schematic of two-dimensional gas separation/ion detection for O_2, CH_4, CO_2, and N_2O in time and *m/z* domains using a short column for rough separation and high-resolution mass spectrometry (MULTUM). O_2, CH_4, and N_2O are detected as O^+, CH_4^+, and N_2O^+ with ion counting, respectively, whereas CO_2 is detected as CO_2^+ with waveform averaging. In chromatographic domain, CO_2 and N_2O are not fully separated, but in *m/z* domain, residual contributions of CO_2^+ and N_2O^+ are fully separated by high mass resolving power of MULTUM.

https://doi.org/10.5194/amt-2019-389
Preprint. Discussion started: 17 March 2020

Atmospheric Measurement Techniques Discussions

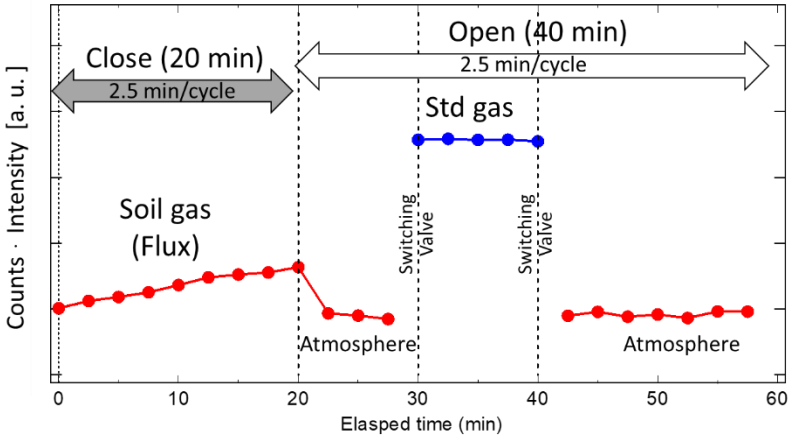

Figure 3. Example sequence of flux measurement conducted over 1 h and continued during field and laboratory flux observations. The flux chamber is closed for the first 20 min of flux measurement. During the remaining 40 min, the chamber is open and standard and atmospheric gas measurements are conducted for system stability verification and calibration. (Std, standard)

https://doi.org/10.5194/amt-2019-389
Preprint. Discussion started: 17 March 2020

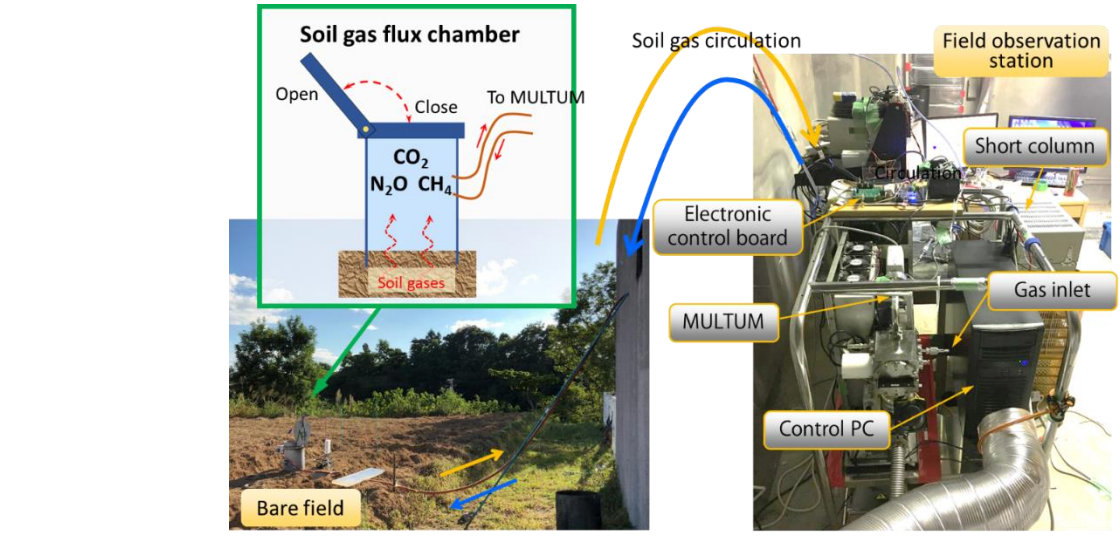

Figure 4. Instrument setup during field flux observation at University Farm of Ehime University (Matsuyama-shi, Ehime, Japan).

https://doi.org/10.5194/amt-2019-389
Preprint. Discussion started: 17 March 2020

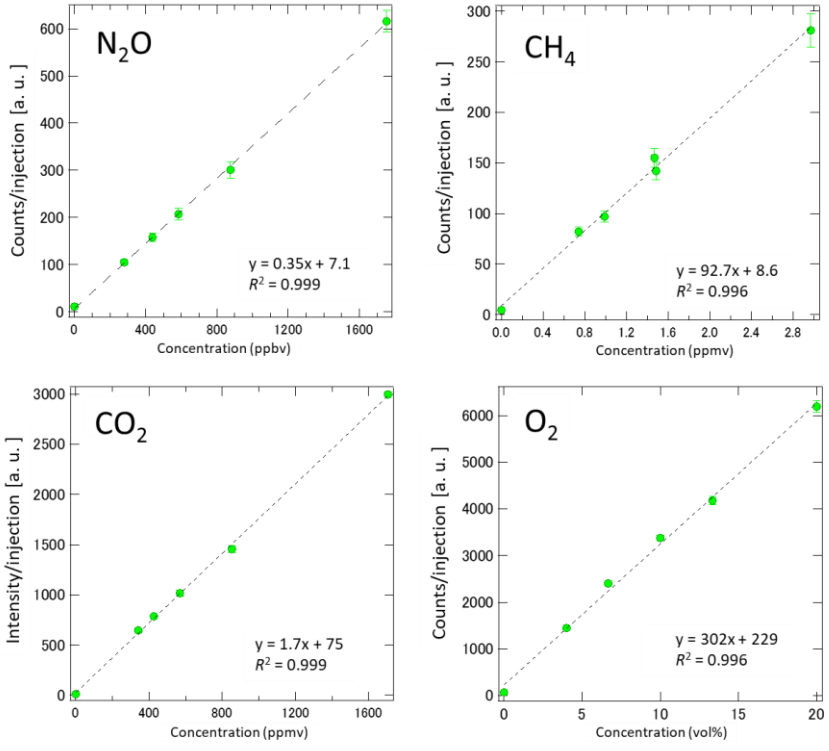

Figure 5. Calibration curves of MULTUM by introducing standard gases of N_2O, CH_4, CO_2, and O_2 mixture in ultrapure N_2. The coefficients of determination (R^2) for linear regression were all above 0.996 regardless of concentration for all the gases based on 10 replicate injections.

https://doi.org/10.5194/amt-2019-389
Preprint. Discussion started: 17 March 2020

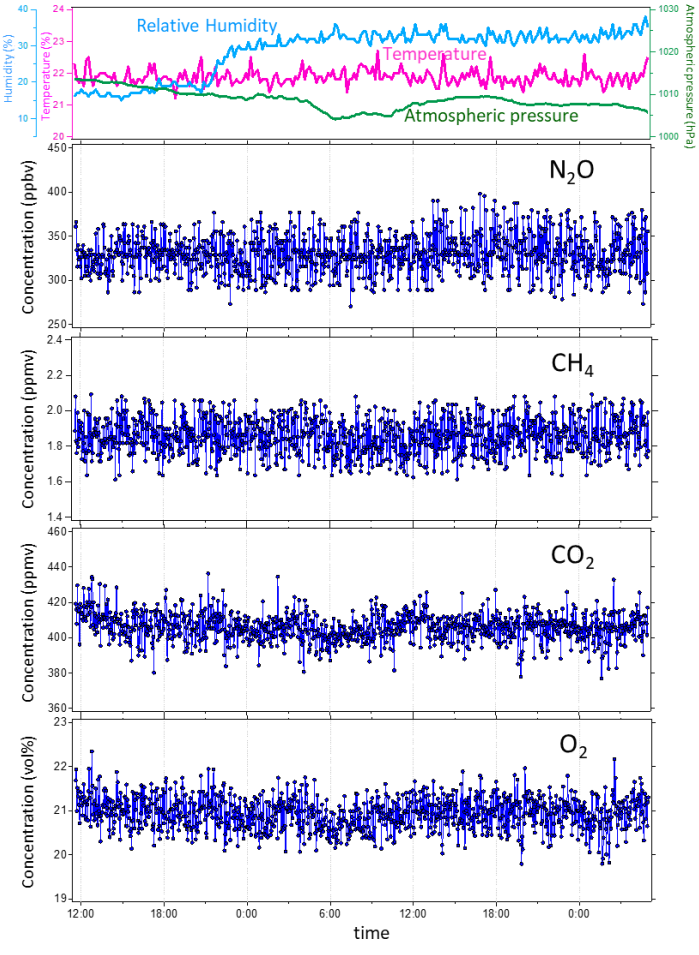

Figure 6. Continuous measurements of atmospheric N_2O, CH_4, CO_2, and O_2 in laboratory with soil chamber opened. Every 2.5 min, concentrations of the four gases were observed. The blue dots indicate individual data points. Top panel: the variations of atmospheric conditions during the laboratory measurement (atmospheric temperature, pressure, and relative humidity

https://doi.org/10.5194/amt-2019-389
Preprint. Discussion started: 17 March 2020

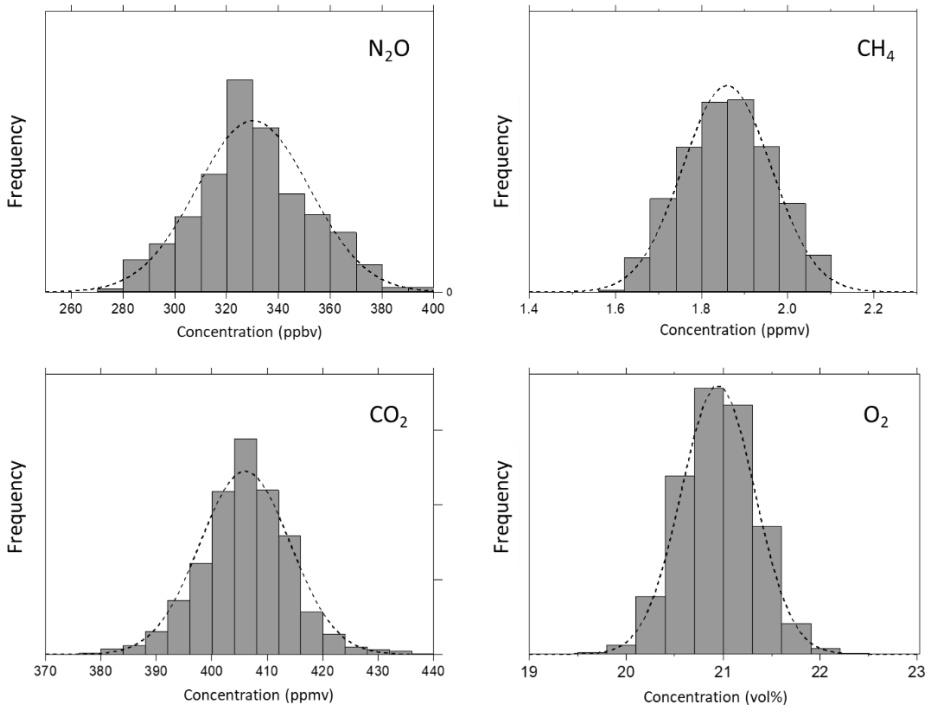

Figure 7. Frequency distributions of measured atmospheric concentrations of N_2O, CH_4, CO_2, and O_2 (994 samples) during laboratory atmospheric air measurement with MULTUM-soil chamber system. Gaussian distributions are plotted as dashed lines for comparison.

https://doi.org/10.5194/amt-2019-389
Preprint. Discussion started: 17 March 2020

Atmospheric Measurement Techniques Discussions

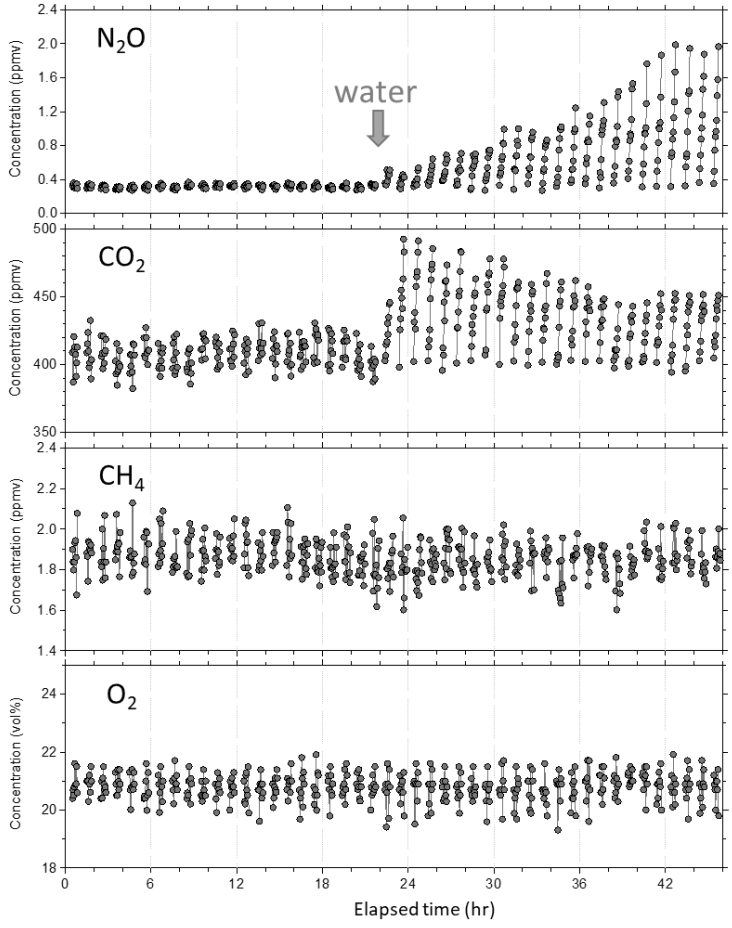

Figure 8. Example of continuous simultaneous flux measurement of N_2O, CH_4, CO_2, and O_2 in laboratory on simulated field. After 22 h, water (3 L) was sprayed on the soil surface. Immediately after the water addition, emission of N_2O and CO_2 began to change in different ways. For CH_4 and O_2, no flux beyond their minimum quantitative fluxes was observed throughout the flux measurement.

https://doi.org/10.5194/amt-2019-389
Preprint. Discussion started: 17 March 2020

Atmospheric Measurement Techniques Discussions

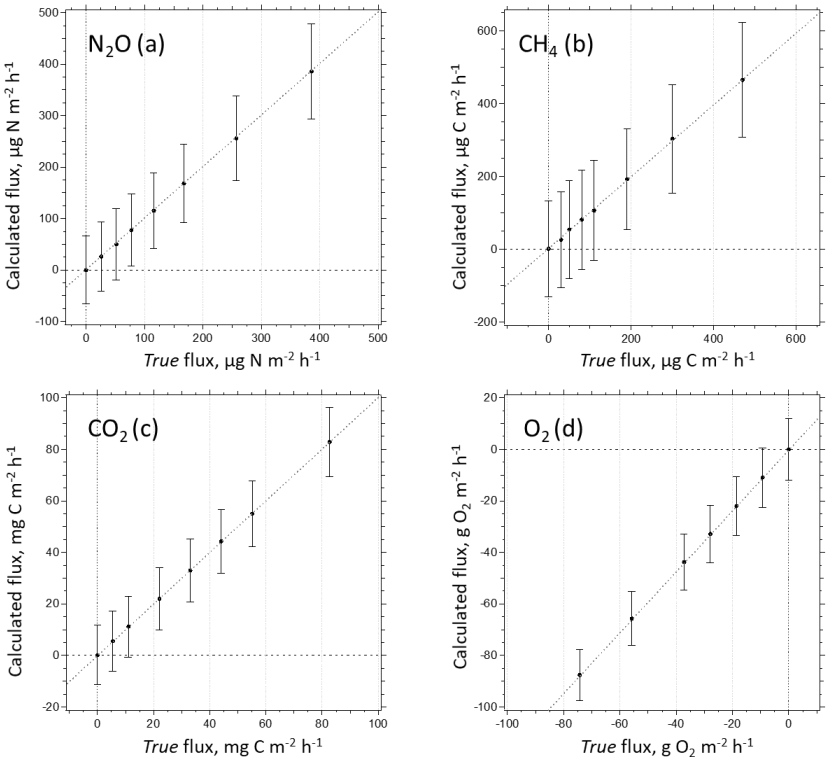

Figure 9. Relationship between true and simulated measured fluxes and uncertainties in simulated flux measurement and determination to estimate minimum quantitative flux (MQF). The error bars in the figures represent uncertainties of fluxes (two standard deviations) determined from simulated flux measurements. (a) N_2O, (b) CH_4, (c) CO_2, and (d) O_2.

https://doi.org/10.5194/amt-2019-389
Preprint. Discussion started: 17 March 2020

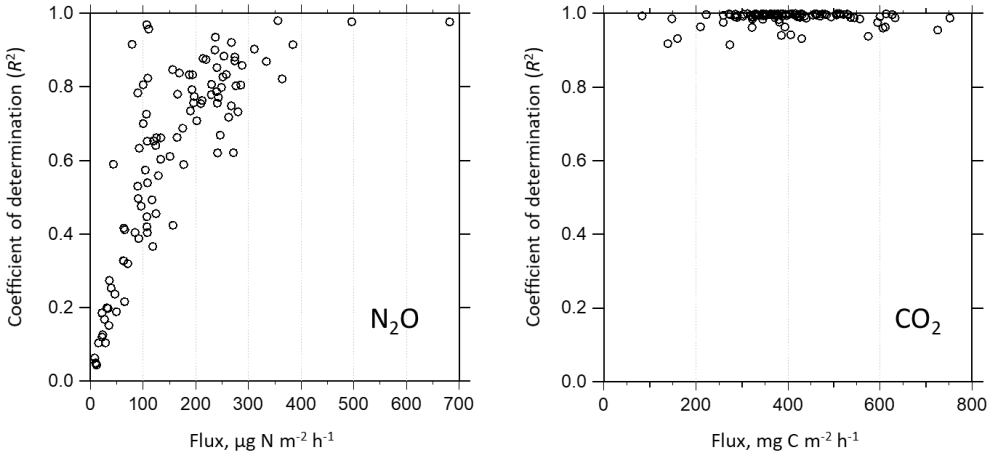

Figure 10. Relationship between determined fluxes and coefficient of determinations (R^2) in the linear regression to derive corresponding slopes (fluxes) from nine consecutive gas concentration observations per flux measurement during field flux observation at Ehime University.

https://doi.org/10.5194/amt-2019-389
Preprint. Discussion started: 17 March 2020

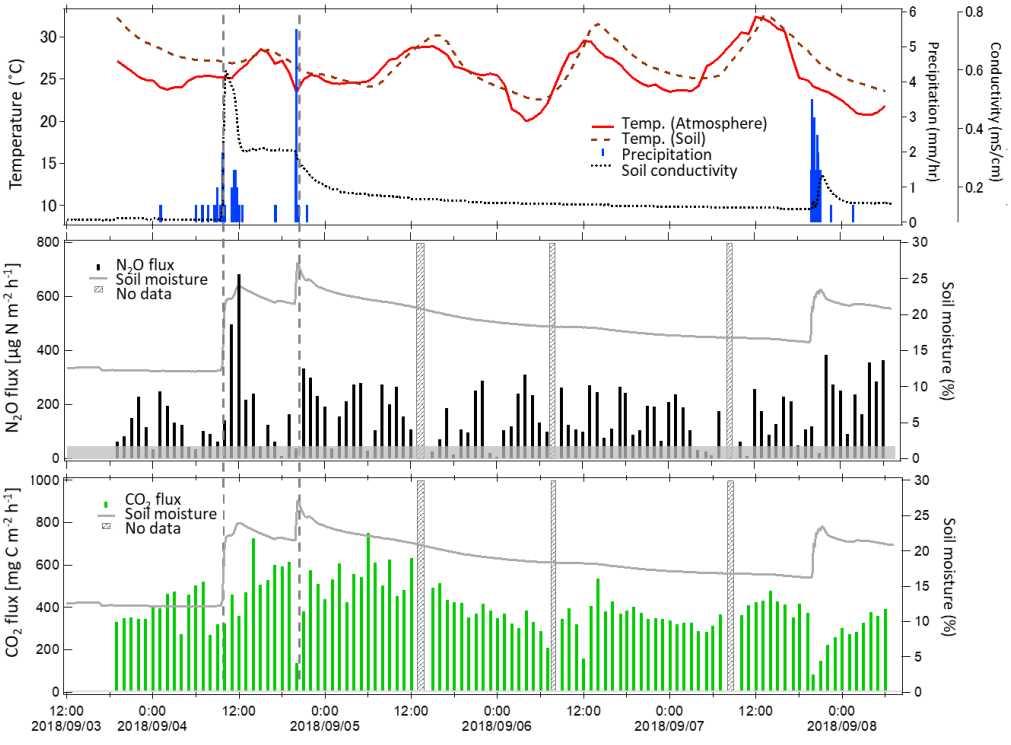

Figure 11. Temporal variations of observed N_2O and CO_2 fluxes at the University Farm of Ehime University during field flux observation in September 20